Re-Interpretation of the ^{2}H(d,pp)nn Reaction at 80 MeV

R.E. Warner

Leeman et al.[1] used the 80 MeV deuteron beam from the University of Maryland Cyclotron to induce ^{2}H(d,pp)nn double breakup. They compared their data with PWBA predictions assuming a double spectator process (DSP) in which the target neutron remained at rest in the lab while the projectile neutron maintained the beam velocity. In general their fits were unsatisfactory, and they speculated that the double-spin-flip process

$$d + d \rightarrow d^*(^1S_0) + d^*(^1S_0) \qquad (1)$$

contributed to the yield at one of their geometries.

In contrast, I have obtained good fits to all their reported data by assuming final-state interactions (FSI) between both final n-p pairs and ignoring the DSP. Both the Wigner and $V_{\sigma\tau}$ parts of the N-N force lead to double breakup. Therefore, the four-body final state is taken to be an incoherent mixture of two $^1S_0$ (singlet deuteron) and two $^3S_1$ n-pairs.

Watson[2] showed that, when a final-state n–p pair have small enough relative momentum k, their wave function is

$$\psi_{np} = \frac{e^{-i\delta}\sin\delta}{k} \; f(r) \qquad (2)$$

where δ is the elastic scattering phase shift and r is their separation. Thus the square modulus of our matrix element contains a factor $(\sin^2\delta/k^2)$ for each n-p pair. The yield $y(E,\theta)$ for detecting two protons with equal lab energies E and at equal coplanar lab angles θ is

$$y(E,\theta)=A\int(\sin^2\delta_{1,L}\sin^2\delta_{1,R}+\sin^2\delta_{3,L}\sin^2\delta_{3,R}) \times \frac{\rho_F}{k^2_L k^2_R}\sin\alpha d\alpha d\phi \qquad (3)$$

where ρ_F is the density of final states and (α,ϕ) are the emission angles of one neutron in the n-n c.m. system. The subscript L(R) designates the proton detected on the left (right) of the beam and the neutron emitted nearest to it. The singlet and triplet n-p phase shifts δ_1 and δ_3 were computed from the currently accepted[3] n-p effective range parameters. The normalization A and triplet-to-singlet ratio η were the only parameters adjusted while fitting 48 data points.

The data, my FSI predictions, and the original DSP fits are shown in the accompanying figure. Generally the FSI fits are superior; in particular they predict the peak center more accurately at $\theta = 36.5^o$, where Leeman et al.[1] attributed the discrepancy between observations and DSP predictions to multiple scattering. The best

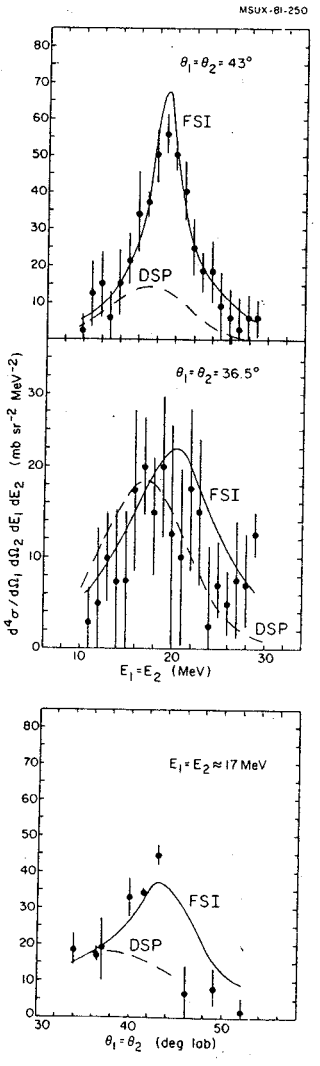

Data for ^{2}H(d,pp)nn reaction at 80 MeV, with original predictions assuming double spectator processes (DSP) and our predictions assuming final-state interactions (FSI) between both final n-p pairs.

FSI fit was obtained with η = 4. Since η would equal 9 if spin statistics alone determined the yield, we find that the singlet dueteron state has greatest intrinsic strength but the $^3S_1$ states also participate. Our best fit has a χ^2-per point, χ^2_1, of 1.15. One measured datum (E = 17 MeV, $\theta = 43^o$) has different values of 37 and 44 mb/(sr^{2}MeV^2) in the upper and lower panels, respectively, of the figure. If both were set at the lower value χ^2_1 would drop to 0.98.

At this bombarding energy it is hard to distinguish the contributions of the DSP and the $^3S_1$ FSI, both of which have broad energy depend-

ence. Measurements with the 160 MeV deuteron beam from the MSU superconducting cyclotron will help to establish the relative importance of the two mechanisms. A comment on this work has been accepted for publication in Physical Review C.

---

1. B.Th. Leeman, H.G. Pugh, N.S. Chant and C.C. Chang, Phys. Rev. C17 (1978) 410.
2. K.M. Watson, Phys. Rev. 88 (1952) 1163.
3. H. Guratzsch, B. Kuhn, H. Kumpf, J. Mosner, W. Neubert, W. Pilz, G. Schmidt and S. Tesch, Nucl. Phys. A342 (1980) 239.

Extended PWBA Treatment of the ^{6}Li + ^{6}Li→2α+ 2d Reaction

R.E. Warner

Recently d-d and α-α double coincidence energy spectra from the above reaction were measured[1] at the Chalk River Tandem Accelerator. Experimental geometries were selected which permitted (but did not require) the two undetected final nuclei to be spectators to the reaction; i.e., the cluster from the target could stay at rest in the lab while the undetected projectile cluster maintained the beam velocity. Striking evidence for double spectator pole (DSP) behavior was observed in 20 of the 21 spectra which were obtained. The observed peak centers in both α-α and d-d coincidence spectra agreed well with those predicted by a simple kinematic argument but their widths were often five or more times smaller than those predicted from the momentum distribution of α+d clusters in ^{6}Li. It was verified that these enhancements did not result from phase space, a final-state interaction, or sequential decay of levels in ^{4}He, ^{6}Li, or ^{8}Be.

We have extended the PWBA theory used in interpreting our original results, to try to explain the abnormally small widths of the observed peaks. First, we showed that the PWBA (through comparison with PWBA calculations of the d-d and α-α elastic scattering cross sections) correctly predicts the approximate strengths of the peaks, reinforcing our belief that they result from the DSP mechanism. Results for those experimental conditions most closely approximating quasi-free scattering are given in Table I. The tabulated cross sections are those at the peak of the distribution; net measured cross sections were obtained by subtracting the continua which underlie the peaks. Total yields are proportional to the product of $d^4\sigma$ and peak widths. Since the latter are about five times as great for the predictions as for the measurements, the predicted d-d coincidence yields are quite close to those measured. The α-α measurements and predictions are quite close at the lowest bombarding energy E_o, but the predictions increase and the measured values decrease with increasing E_o.

Table I. Measured and predicted ^{6}Li+^{6}Li double breakup cross sections.

E_o (MeV)	(deg)	Type	$d^4\sigma$ (mb/sr^2 MeV^2) Measured	Predicted
36.4	41.0	α-α	6.4	1.6
39.4	41.4	α-α	5.4	4.4
43.0	41.7	α-α	4.8	6.7
46.6	42.0	α-α	2.7	7.0
36.4	41.0	d-d	2.0	0.55
39.4	41.4	d-d	2.1	0.52
43.0	41.7	d-d	1.2	0.51
46.6	42.0	d-d	1.6	0.45

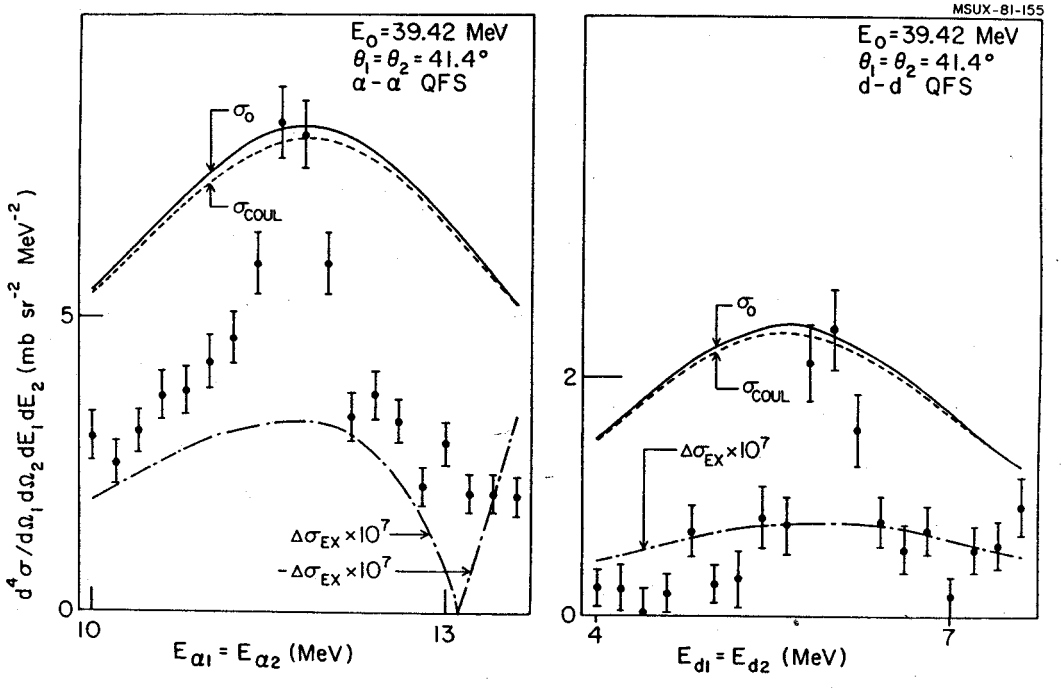

Fig. 1. Coulomb and exchange corrections to the ^{6}Li + ^{6}Li→ 2α + 2d PWBA cross section.

Several improvements were made to the original PWBA interpretive model. The relative momenta of the α+d clusters at the DSP peaks is so small that they must tunnel through a Coulomb barrier of length ~20 fm. Therefore, Coulomb cluster wave functions were used for computing the momentum wave functions of the clusters. The result (curves labelled σ_{COUL} in Fig. 1) is a slightly broader predicted peak than that predicted for a nuclear Woods-Saxon well with Coulomb effects neglected (curves labelled σ_o). This increased width results from the greater roughness of the Coulomb spatial wave function, which depletes the low-momentum components of the momentum wave function.

Exchange effects were incorporated first by symmetrizing the matrix element for exchange of identical bosons, all of which were treated as point particles. The curves labelled $\Delta\sigma_{EX}$ in Fig. 1 show the corrections due to this effect; they are seen to be quite negligible. Deuteron structure effects were then included by treating the deuteron not as a single particle, but as two nucleons whose spatial wave function was the sum of three gaussian functions.[2] The additional matrix elements thus introduced also had negligible effects on our predictions. These matrix elements were found to be not of spectator type; thus, in any model giving larger exchange amplitudes, still broader peaks will be predicted.

The range r_o of the participant interaction potential was varied because it is one of the few adjustable parameters in the extended PWBA theory, and because the effects of this potential may crudely simulate those of distorted waves for the participants, which would be much harder to incorporate. The predicted peak widths were still too large and nearly independent of r_o. However, when $r_o > 1$ fm, the predicted peak center shifted appreciably below the observed one. Therefore, a δ-function interaction potential was used throughout the other calculations.

A paper describing this work was submitted to Nuclear Physics A.

---

1. R.E. Warner, G.C. Ball, W.G. Davies, and J.S. Forster, Nuclear Physics A365 (1981) 142.
2. W.T.H. van Oers and I. Slaus, Phys. Rev. 160 (1967) 853.

Mass of the Lowest T=2 Levels in ^{8}Be and ^{8}Li

A. Ledebuhr, R.G.H. Robertson and L.W. Robinson

The A=8 isobaric quintet is of special interest in that it is the only completed quintet which shows a slight deviation from the quadratic form of the isobaric multiplet mass equation (IMME),

$$\Delta M = a + bT_z + cT_z^2$$

Additional cubic (dT_z^3) and quartic (eT_z^4) terms have coefficients 3.6±2.7 and 2.6±2.1 keV respectively.[1] Isospin mixing in the T_z=0 member of the multiplet (^{8}Be) has been suggested as a possible cause for part of this deviation.[2] Because of the approximate mirror symmetry of quartets, mixing with T=½ states contributes chiefly to a T_z^2 term whereas in quintets mixing with T=0 or 1 states immediately causes a T_z^4 dependence. To understand these effects further, a remeasurement of the T=2 levels in ^{8}Be and ^{8}Li is in progress here at Michigan State University. A 45 MeV proton beam from the MSU Cyclotron bombarded a 114 μg/cm^2 target of 94% enriched ^{10}BeO on a 1 mg/cm^2 Pt backing.[3] ^{3}He and t particles from the reactions ^{10}Be(p,^{3}He)^{8}Li and ^{10}Be(p,t)^{8}Be were recorded on 20-inch photographic plates mounted in the focal plane of the Enge split-pole spectrograph. Deuterons were recorded simultaneously with the tritons and will be used as calibration lines for the triton peak. An electrostatic deflector positioned in the gap of the spectrograph gave a vertical displacement proportional to m/q which effectively separated the different particles. Two sets of exposures were made at laboratory angles of 8°, 9° and 10°. We are in the process of scanning these plates and it is expected that masses with an accuracy of 1 to 2 keV will be achieved. This will allow a check on the previous measurements as well as a further test of the IMME.

---

1. R.G.H. Robertson, E. Kashy, W. Benenson and A. Ledebuhr, Phys. Rev. C 17, 4 (1978).
2. R.G.H. Robertson, W. Benenson, E. Kashy and D. Mueller, Phys. Rev. C 13, 1018 (1976).
3. D.R. Goosman, Nucl. Instrum. Methods 116, 445 (1974).

Production of 6.13 MeV gamma rays from the $^{16}O(p,p'\gamma)^{16}O$ Reaction at 23.7 and 44.6 MeV

J. Narayanaswamy, P. Dyer, S.R. Faber[+] and Sam M. Austin

Laboratory measurements of gamma-ray production cross sections and Doppler broadened line shapes over a broad range of projectile energies are required for the interpretation of astrophysical gamma-ray line spectra.[1-4] One can, in principle, calcualte the gamma production cross section from inelastic proton and alpha scattering data and gamma-ray branching rations. However, because of the uncertainties in the contribution of cascade processes to gamma-ray production and the uncertainties in calculating the broadening effects, it is desirable to measure the gamma-ray yields directly. We have measured yields of 6.13 MeV gamma rays from the reaction $^{16}O(p,p'\gamma)^{16}O$ at incident lab proton energies of 23.7 and 44.6 MeV. Our results agree at the lower energy with the cross sections of Dyer et al.[1] but disagree with those of Zobel et al.[5]

The experimental set up using a gas target and two Ge(Li) detectors has been described elsewhere.[12] The 6.13 MeV line arises from an E3 transition, and determination of total cross section requires measurements at atleast 3 angles. The geometry of the set-up permitted measurements between 45° and 157° relative to the incident beam. At each angle, data were acquired with the cell filled with gas and with the cell empty, and energy spectra were recorded with a sigma 7 computer. Detector efficiency was measured with a calibrated source,[6,7] of 6.13 MeV gamma rays ($^{238}Pu + ^{13}C$) in the same source detector geometry as that of the experimental runs. Typical spectra (after subtracting the cell contribution) are shown in Fig. 1. The analysis was complicated by the overlap of the broad 6.13 MeV full energy peak (FEP) with the double escape peak (DEP) of the 7.12 MeV line from ^{16}O, at 6.10 MeV. The latter peak (making about a 10% contribution to the area) had to be subtracted before extracting areas under the full energy peak. It was done as follows.

From the sharp-peaked spectrum of the calibrated source of 6.13 MeV gamma rays, we extracted relative areas of the FEP and DEP. We also obtained parameters to describe the behavior of the compton background above and below the DEP. The DEP was parameterized by the sum of a gaussian and a Woods-Saxon type function. This was found to reproduce the Sharp DEP excellently. We then estimated a FWHM and height from the FEP of the 7.12 MeV line at each angle, obtained the shape of the DEP using the above source parameters, position being determined from the energy calibration, and made a channel by channel subtraction. The subtraction contributes negligible error to the final 6.13 MeV yield.

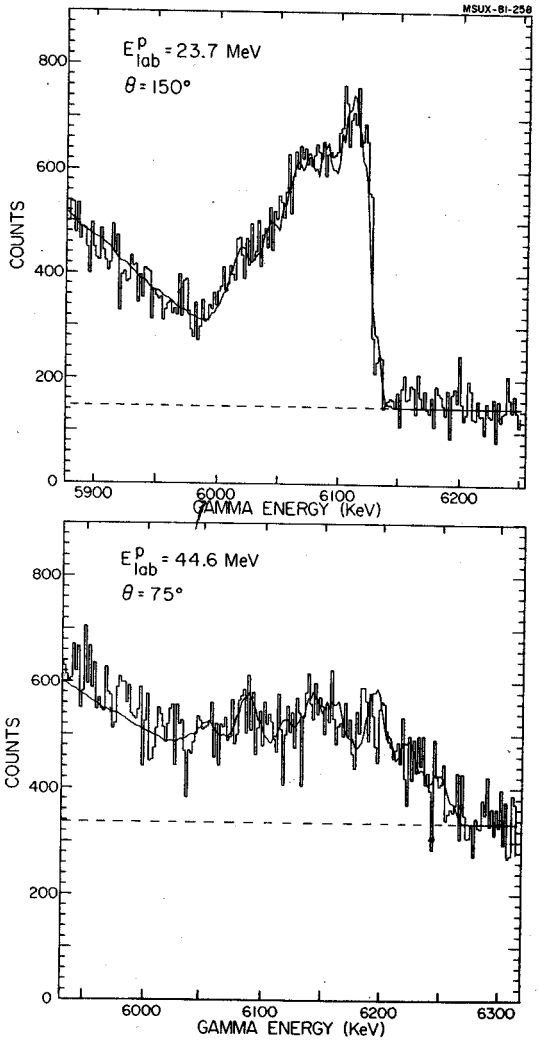

Fig. 1. Spectra of gamma rays with empty cell background and the 7.12 MeV DEP subtracted. The remaining background is assumed to be flat and with the (fitted) magnitude shown in the highest channels. The curve is the result of the fit using unsmoothed reference peaks derived from the $^{238}Pu + ^{13}C$ source.

For extraction of areas under the broad 6.13 MeV peaks, a reference peak shape was created by adding four off set spectra from the $^{238}Pu + ^{13}C$ source (to create a broader line). Five to nine such reference peaks were then used to fit the data, using a modified version of Bevinton's routine 'CURFIT'.[8] Peak positions and amplitudes were then varied to minimize χ^2. This procedure permitted a consistent treatment of the compton edges for these broad lines; otherwise a detailed fit of the complex peak structure is unnecessary to obtain the gamma-ray production cross sections. The angular distribution of gamma rays relative to the beam direction is

$$\frac{d\sigma}{d\Omega}(\theta) = \sum_{\ell=0}^{L} P_\ell(\cos\theta) \quad \text{even } \ell$$

The quantity L is the smaller of the two values- (a) twice the spin of the decaying state (b) twice the multipolarity of the gamma ray.[9] For 6.13 MeV gamma rays, L = 6. The total cross section depends on a_o only and is given by $\sigma_{tot} = 4\pi a_o$. We fit the observed differential cross section with a sum of P_0, P_2, P_4 and P_6, varying the a_ℓ's to minimize χ^2. Table I lists the resulting coefficients (with statistical errors). Systematic and statistical errors added in quadrature gave overall uncertainties in the total cross section of about 10% and 12% at 23.7 and 44.6 MeV respectively. The lab to C.M. frame transformation of angles and cross sections was not carried out, as the required correction was less than 1%.

Table II and Fig. 2. show total cross sections derived from the present experiment and from previous work based on γ-ray or (p,p') measurements at or near the proton energies of this work.

Our cross section at 23.7 MeV compares favorably with the value measured by Dyer et al.[1] at 23 MeV. The (p,p') cross sections of Austin et al.[10] and Bayer[11] when compared to our measurements indicate the increasing contribution from cascades especially at the higher energy. Zobel et al.[5] measured gamma rays in the range 6.1 - 6.3 MeV at incident proton energies of 16, 33, 56 and 100 MeV. They assumed the yield to be isotropic and measured at one angle only. There is a strong discrepancy indicated between their results and our measurements. Our angular distribution coefficients indicate that the assumption of isotropy, although reasonalbe at energies above 40 MeV, is not valid at the lower energies. Extension of this type of work to include higher proton and alpha energies and more targets is useful not only for gamma-ray astronomy but also, as discussed by Zobel et al.[5] for computing the contribution of secondary gamma rays to radiation dose rates produced by charged particles in space.

Table I. Legendre polynomial coefficients for gamma-ray angular distribution from $^{16}O(p,p'\gamma)^{16}O$.

E^p_{lab}(MeV)	a_o $\frac{mb}{sr}$	a_2 $\frac{mb}{sr}$	a_4 $\frac{mb}{sr}$	a_6 $\frac{mb}{sr}$
23.7	4.68±0.12	1.74±0.29	-0.03±0.52	-0.94±0.60
44.6	3.21±0.20	-0.32±0.74	-0.28±1.06	-1.18±1.02

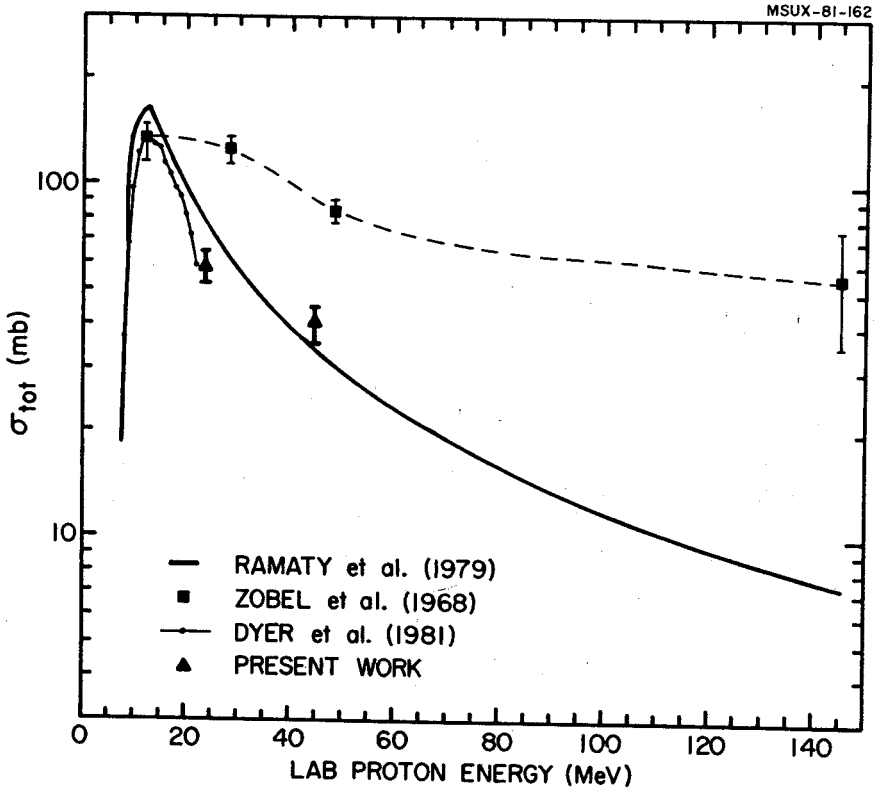

Fig. 2. Total cross section σ_{tot} vs. lab proton energy. Heavy solid line: estimate by Ramaty et al. (Ref. 2). Filled circles: cross sections measured by Dyer et al. (Ref. 1), averaged over 1-MeV-wide energy bins; solid line connects the points. Filled squares: Measurements by Zobel et al. (Ref. 5), dashed line drawn to guide the eye; gamma rays in the range 6.1-6.3 MeV are included. Filled triangles: Present work.

Table II. Comparison of p + ^{16}O cross sections.

Reference	σ_{tot}(mb)[f]			
	E^p_{lab}	25 MeV	E^p_{lab}	44 MeV
Dyer et al.[a]		58±9		
Ramaty et al.[b]		79		35
Zobel et al.[c]		124±10		86±6
Austin et al.[d]		60±2		26±1
Bayer[e]		54±5		30±6
Present work		58.9±6.2		40.4±4.9

[a]Reference 1: (p,p'X); 6.13 MeV -rays; E^p_{lab} = 23 MeV.

[b]Reference 2: Estimated from (p,p') data, -ray cross sections, and branching ratios; 6.13 MeV γ-rays; E^p_{lab} = 23.8 and 44.7 MeV.

[c]Reference 5: (p,p'γ); 6.1-6.3 MeV -rays; E^p_{lab} = 28.2 and 48.3 MeV; measured at =135°, assumed isotropic yield.

[d]Reference 10: (p,p') to 6.05 plus 6.13 MeV states; E^p_{lab} = 23.4 and 43.1 MeV.

[e]Reference 11: (p,p') to 6.13 MeV state; E^p_{lab} = 24.6 and 40.1 MeV.

[f]Errors quoted here are combination of statistical and systematic errors added in quadrature.

+ Present address: Bell Laboratories, 6H 338, Warrenville and Naperville Roads, Naperville, IL 60566

1. P. Dyer, D. Bodansky, A.G. Seamster, E.B. Norman, and D.R. Maxson, Phys. Rev. C 23, 1865 (1981).
2. R. Ramaty, B. Kozlovsky, and R.E. Lingenfelter, Astrophys. Jour. Supp. Serv. 40, 487 (1979).
3. R.E. Lingenfelter and R. Ramaty, Phys. Today 31, No. 3, p. 40 (1978).
4. NASA Technical Memorandum Report NO. 79619, edited by T.L. Cline and R. Ramaty, 1978.
5. W. Zobel, F.C. Maienschein, J.H. Todd, and G.T. Chapman, Nuclear Science and Engineering 32, 392 (1968).
6. Source manufactured by Laboratoire de Metrologie des Rayonnements Ionisants, Saclay, France and on loan from Argonne National Laboratory, Argonne, IL.
7. K.W. Geiger and L. Van der Zwan, Nucl. Instr. Methods 157, 199 (1978).
8. P.R. Bevington, Data Reduction and Error Analysis for the Physical Sciences, (McGraw-Hill, 1969), p. 237.
9. R.M. Steffen and K. Alder, The Electromagnetic Interaction in Nuclear Spectroscopy, edited by W.D. Hamilton (North Holland, Amsterdam, 1975), p. 505.
10. Sam M. Austin, P.J. Locard, S.N. Bunker, J.M. Cameron, J. Reginald Richardson, J.W. Verba and W.T.H. van Oers, Phys. Rev. C 3, 1514 (1971).
11. D. Bayer, unpublished Ph.D. Thesis, Michigan State University (1970).
12. Physical Review C to be published.

Energy Levels of ^{60}Ni

M.S. Curtin, R.M. Ronningen, J.A. Nolen, R.C. Melin,* S. Raman** and H. Nann***

The ^{59}Ni(d,p) reaction at 20 MeV was used for a detailed study of energy levels and excited state yields in ^{60}Ni.[1] Wire counter and photographic plate data were collected. Calibration energies for states in ^{60}Ni were obtained from (n,γ) and (p,p') reactions.[2] The low excitation energy plate data is shown in Fig. 1. The numbered state excitation energies are given in Table I. Above approximately 6 MeV excitation energy, the high density of populated states made state identification impractical.

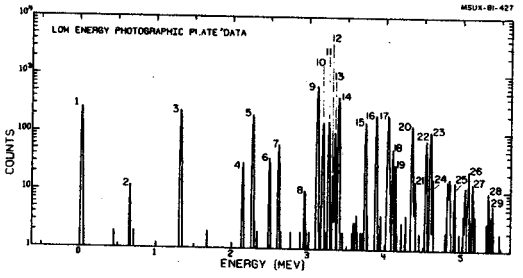

* Bell Telephone Laboratories, Allentown, PA
** Oak Ridge National Laboratory, Oak Ridge, TN
*** Indiana University, Bloomington, IN

1. M.S. Curtin et al., Annual Report (MSU) 1979-80.
2. S. Raman et al., to be published.

Table I

Peak	Fit Energy (keV)	
1	6.77	
2	656.16	Impurity
3	1225.45	
4	2158.41	
5	2285.70	
6	2506.22	
7	2526.67	
8	2960.02	Impurity
9	3122.77	
10	3191.92	
11	3267.62	
12	3317.19	
13	3345.15	
14	3391.95	
15	3733.14	
16	3869.85	
17	4019.00	
18	4076.81	
19	4109.42	
20	4317.76	
21	4352.86	
22	4493.02	
23	4546.21	
24	4575.02	
25	4844.10	
26	5010.53	
27	5066.33	
28	5264.00	
29	5309.59	

Study of $^{56}Fe(d,^2He)$ and Similar Reactions

K. Beard, G. Bertsch, E. Kashy, R.E. Warner,* B.H. Wildenthal, D. Friesel** and H. Nann**

We have planned a series of $(d,^2He)$ reaction studies, starting with the experiment, $^{56}Fe(d,^2He)^{56}Mn$, which has been awarded time at IUCF; the incident energy will be 90 MeV, and the coincident protons from ^2He will be detected by two counter telescopes. Later studies will utilize the 160 MeV deuteron beam from the MSU Superconducting Cyclotron and a multi-wire proportional counter (MWPC) in the focal plane of the Enge split-pole spectrograph.

Since the di-proton (or ^2He) is in a T=0, ^1S_o state, the $(d,^2He)$ reaction should enhance $\Delta L=0$, $\Delta S=1$, $\Delta T=1$ transitions. Therefore it is particularly suitable for populating "M1" states when the target is even-even. Transitions with $\Delta L=0$ can be identified by their steeply-forward-peaked angular distributions.

The first experiment will be a measurement of the strengths and excitation energies of the ^{56}Mn "M1" states, via the $^{56}Fe(d,^2He)^{56}Mn$ reaction. These data may determine which of two mechanisms[1] blasts off the mantle of a collapsing supernova, permitting the core to evolve into a neutron star. These competing mechanisms are neutrino production during electron capture, and the shock wave induced by compression of the core to super-nuclear densities. Along with these measurements, we will do a calibration study of the $^{12}C(d,^2He)^{12}B$ reaction to verify the angular distribution and the spectrum of p-p relative energies, ϵ_{pp}.

Other studies on our list include the identification of T=2 states in ^{26}Mg, the spectroscopy of neutron-rich nuclei, the shape of the ϵ_{pp}, spectrum for small ϵ_{pp}, and the mechanism of the $^2H(d,pp)nn$ reaction.[2]

We have made calculations of the ϵ_{pp}-spectrum and the coincidence detection efficience of both proposed detection systems, using the Watson-Migdal[3] theory of final-state interactions. These show that, for each proton entering one counter telescope or the spectrograph entrance aperture, we can detect about 5% of the coincident protons for those pairs having $\epsilon_{pp} \lesssim 1$ MeV. We expect that essentially all such pairs will be in s-states, since p- and higher ℓ-waves contribute less than 0.1% of the elastic p-p scattering in this energy range.[4] This assumption can be tested by measuring angular distirbutions of the observed transitions for different cuts in ϵ_{pp}.

The ϵ_{pp}-spectrum from ^2He has its peak at about 0.3 MeV, while typical individual proton energies will be ~40 MeV at IUCF. Thus the opening angle for ^2He decay is small and the two counter telescopes will have a 4.5^o included angle. Each telescope will include a 450 mm thick, 450 mm^2 Si transmission counter; a 15 mm thick, 450 mm^2 Ge stopping counter; and a 250 mm^2 collimator 55 cm from the target. The p+p summed energy spectrum determines the residual nucleus excitation E_x. Taking into account intrinsic counter resolution, beam quality, target thickness, kinematic broadening, and the width of the ϵ_{pp} spectrum, we expect a resolution of 0.24 MeV (FWHM) in E_x for the $^{56}Fe(d,^2He)^{56}Mn$ reaction.

The transmission MWPC, planned will extend about 30 cm along the spectrograph focal plane and will have a ~.9 mm wire spacing and achieve ~60 keV resolution. The anode wires will be held at ground potential and connected to the chamber cards of a Le Croy PCOSII system, which provides the digital addresses of wires whose signals exceed a chosen threshold. The chamber cards will be mounted very close to the MWPC in a gas box, in order to minimize noise and dissipate heat. Proportional signals are not available from this system, but it is very fast and will allow high count rates. Timing and E signals will be generated by two plastic scintillators behind the MWPC.

The anode wires of the MWPC lay in a horizontal plane. Individual wires make 45^o angles with the focal plane, and are parallel to and above the central particle trajectory. The cathode plane is about 4.5 mm below the plane of the anode wires. The particles will pass between these planes; for central rays, ions will be collected by one or two wires. The gas mixture and operating voltage are not yet chosen, but the construction of a short 32-wire prototype MWPC is in progress.

---

* Permanent address: Oberlin College, Oberlin, OH 44074.
** Collaborator from Indiana University Cyclotron Facility, Bloomington, IN 47401

1. H.A. Bethe, et al., Nucl. Phys. A324 (1979) 487.
2. R.E. Warner, submitted to Phys. Rev. C; see also pp. ( ) of this report.
3. K.M. Watson, Phys. Rev. 88 (1952) 1163.
4. P.S. Signell, private communications.

Observation of M1 Strength by the Inelastic Scattering of 200-MeV Protons

N. Anantaraman, G.M. Crawley, A. Galonsky, C. Djalali,* N. Marty,* M. Morlet,* A. Willis,* J.-C. Jourdain* and P. Kitching**

A new resonance has been observed in the inelastic scattering of 200-MeV protons. Forward peaking of the angular distribution is evidence that $\Delta L = 0$ in this resonance, and the dominance of spin-flipping amplitudes in the effective interaction at 200 MeV implies that $\Delta S = 1$. For an even-even target the transition is one of $0^+ \rightarrow 1^+$.

Although the expected transition strength, M1 strength, has been difficult to find with other reactions[1,2] in nuclei having $A > 50$, in the (p,p') reaction at 200 MeV we have found a concentration of M1 strength in 14 different target nuclei between A = 51 and 100. For ^{90,92,94}Zr a report more detailed than that given here has recently been published.[3] All of our data were taken with the Orsay synchrocyclotron and a large magnetic spectrometer utilizing a computerized electronic ray-tracing detection system. In ^{90}Zr, the resonance has also been seen with 200 MeV protons at TRIUMF.[4]

A spectrum for each of the fourteen targets (except ^{96}Zr) exhibiting the resonance is shown in Fig. 1 or in Fig. 2. These spectra were taken at a scattering angle of 4°. The M1 resonance is the gross-structure enhancement centered around 8 to 10 MeV. The spectra of our heaviest targets- ^{120}Sn, ^{124}Sn, and ^{140}Ce did not obviously show the resonance. Four-degree spectra of these targets are given in Fig. 3. A comment about ^{140}Ce: We had expected it to be a good candidate for the M1 transition, because the simple shell model has its neutron $h_{11/2}$ shell filled and its $h_{9/2}$ shell empty. Analogously, the zirconium nuclei have their neutron $g_{9/2}$ shells filled and their

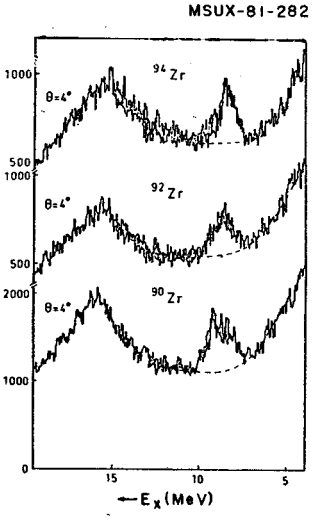

Fig. 1

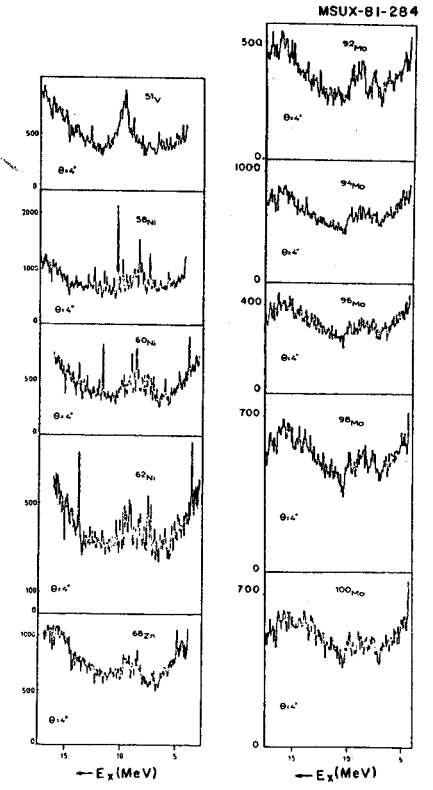

Fig. 2

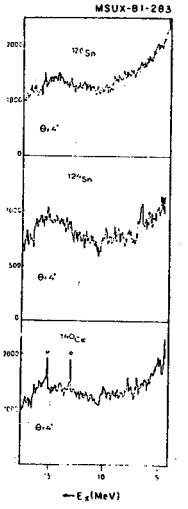

Fig. 3

$g_{7/2}$ shells empty but they do exhibit the spin-flip resonance clearly.

Beyond that already published,[3] our data processing has not reached the stage where we can present angular distributions. However, from Fig. 4, which contains ^{51}V spectra at 3° and at 8°, and from the ^{51}V spectrum in Fig. 2, which

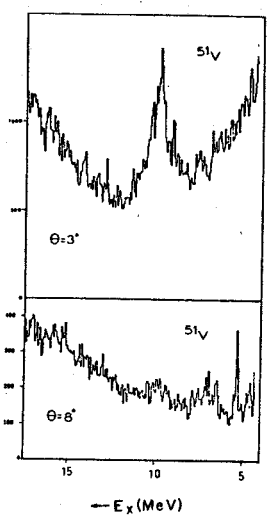

Fig. 4

is for 4°, one can see in a qualitative way that the angular distribution is forward peaked. The sharpness of the resonance in ^{51}V (our only odd-A target) might seem surprising if one thinks that with final states of $J^{\pi} = 5/2^-$, $7/2^-$ and $9/2^-$ in comparison to the even-even targets, where only 1^+ is allowed, one would expect a greater, not a lesser, spreading of the M1 strength. However, the 1^+(e,e') excitation in ^{48}Ca, which lacks the three protons of ^{51}V, is seen[5] in a single peak of width less than 30 keV.

---

* Institut de Physique Nucléaire, Orsay, France.
** University of Alberta, Edmonton, Alberta, Canada.

1. F.E. Cecil, G.T. Garvey, and W.J. Braithwaite, Nucl. Phys. A232, 22 (1974) - the same reaction as here but at 24 MeV, where the spin-flip and non-flip amplitudes are comparable in magnitude and tend to cancel each other.
2. D. Meuer, R. Frey, D.H.H. Hoffmann, A. Richter, E. Spamer and O. Titze, Nucl. Phys. A349, 309 (1980) - ^{90}Zr(e,e'). They report significant M1 strength in only 3 of the many sharp (<40 keV) states excited.
3. N. Anantaraman, G.M. Crawley, A. Galonsky, C. Djalali, N. Marty, M. Morlet, A. Willis, and J.-C. Jourdain, Phys. Rev. Letters 46, 1318 (1981).
4. F.E. Bertrand, E.E. Gross, D.J. Horen, J.R. Wu, J. Tinsley, D.K. McDaniels, L.W. Swenson, and R. Liljestrand, Physics Letters 103B, 326 (1981).
5. W. Steffen, H.-D. Gräf, W. Gross, D. Meuer, A. Richter, E. Spamer and O. Titze, Physics Letters 95B, 23 (1980).

Elastic and Inelastic Scattering of Alpha Particles at 120 and 85 MeV/Nucleon

D.K. Scott, N. Alamanos,* J. Arvieux,* B. Berthier,* B. Bonin,* G. Bruge,* J.L. Escudié,* H. Faraggi,* L. Farvacque,* D. Legrand,* J.C. Lugol,* W. Mittig,* L. Papineau,* M. Beunerd** M. Levine,+ and A.I. Yavin++

The elastic and inelastic scattering of intermediate energy alpha particles is an interesting introduction to future heavy-ion interaction studies with the K = 500 superconducting cyclotron. In the energy range of 50 - 200 MeV/A one expects a transition region where the interaction changes from that of two nuclei as a whole to that of quasi independent nucleons. Both transparency properties of the optical potential and the collective modes of giant resonances are points of interest.

We have carried out measurements of elastic and inelastic scattering of 480 MeV alpha particles on ^{208}Pb, ^{116}Sn and ^{58}Ni, and 340 MeV alpha particles on ^{208}Pb. We used the Saturne accelerator at Saclay, and the SPES I spectrometer followed by a position sensitive detection in the focal plane. At one field setting the system covered an excitation energy range of 28 MeV with a resolution of 300 keV.

Figure 1 shows the elastic scattering angular distributions on ^{208}Pb for 480 MeV and 340 MeV incident energies (the curves drawn are to guide the eye). From the spacing of the minima we deduced an interaction radius and calculated the total cross sections. The results are shown in Fig. 2, together with measurements at lower energies. Our results fall below the geometrical value of $\pi R^2(1 - V/E)$ where R is the interaction radius, V the barrier height and E the center of mass energy; they follow the trend of a Glauber model calcualtion based on the nucleon-nucleon scattering cross section.[1] The implied nuclear transparency amounts to 20% and 25% at 340 and 480 MeV respectively. Detailed studies of optical potential fits to the data are in progress.

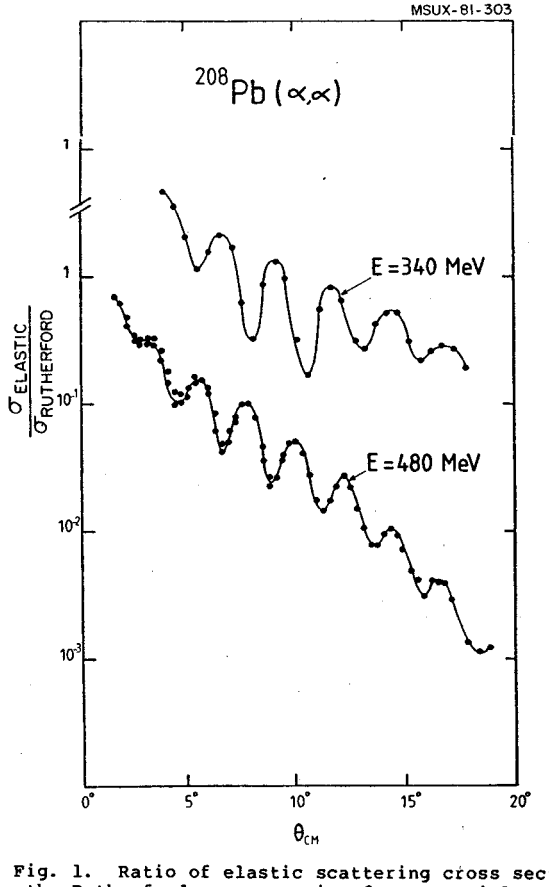

Fig. 1. Ratio of elastic scattering cross section to the Rutherford cross section for α particles on ^{208}Pb at 340 and 480 MeV.

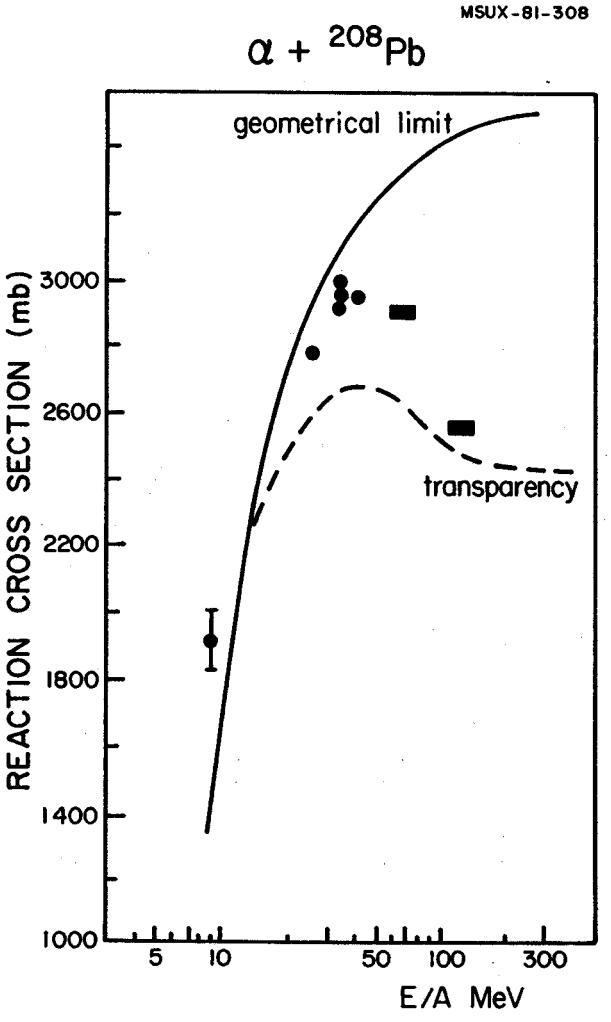

Fig. 2. Reaction cross section for α particles on ^{208}Pb as a function of incident energy. The two highest energy points are deduced from the elastic scattering data of the present work. The theoretical curves are discussed in the text.

The excitation of giant resonances with these high energy alpha beams was also explored. At present three giant resonances are very well established experimentally, viz. the isovector dipole, the isoscalar quadrupole and monopole in many nuclei. Several other giant resonances are predicted and recent experiments with alpha particles provide evidence for the giant octupole and isoscalar giant dipole modes.[2] It was expected that the high energy alpha particle beams would enhance the cross section for resonances and improve the peak to background ratio.

A spectrum for $^{208}Pb(\alpha,\alpha')$ at $\theta = 7^{\circ}$ and $E_{inc} = 480$ MeV is shown in Fig. 3(a). The quadrupole and monopole modes are strongly excited. Some structure in the form of broad peaks is seen at higher energies, both in ^{208}Pb and ^{116}Sn (see Fig. 3(b)). The angular distributions imply that there are at least two components present, with oscillations opposite in phase to those of the quadrupole mode. Further studies of the multipolarities of the observed peaks are in progress.

---

* CEN Saclay, France
** ISN Grenoble, France
\+ Brookhaven National Lab., Upton, L.I., USA
++ Tel Aviv University

1. R.M. DeVries and J.C. Peng, Phys. Rev. C22, 1055 (1980).
2. H.P. Morsch, M. Rogge, P. Turek and C. Mayer-Boricke, Phys. Rev. Lett. 45, 337 (1980).

MSUX-81-307

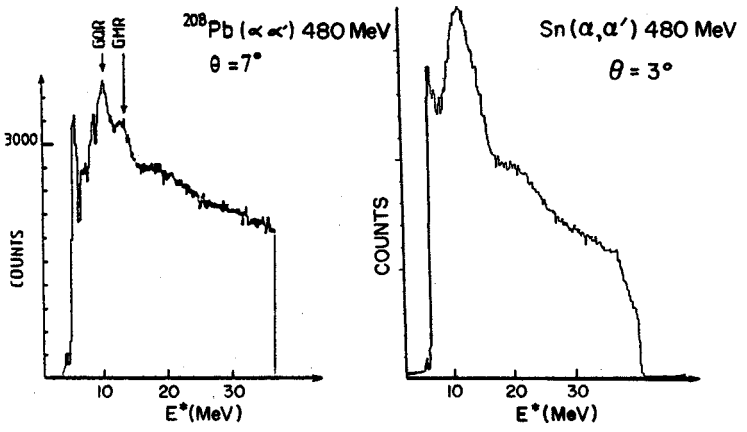

Fig. 3. Energy spectra for alpha particle scattering on (a) ^{208}Pb at 3° and 480 MeV incident energy, and (b) ^{116}Sn at 3.12°.

Determination of the Total Angular Momentum of Deep Hole States from ($\vec{p}$,d) Reactions

J. Kasagi, G.M. Crawley, E. Kashy, J. Duffy, D. Freisel* and S. Gales**

The comparison of predictions of the nuclear response function for single particle (hole) states with experimental data requires a knowledge of the spin-parity of various states or groups of states observed in single nucleon transfer reactions. While the angular distribution is characteristic of the orbital angular momentum ℓ of the transferred particle, knowledge of the total angular momentum (j) is not so readily obtained. We have shown in earlier ($\vec{p}$,d) experiments on ^{120}Sn with polarized protons, that the angular variation of the analyzing power is characteristic of the j- transferred.[1] Both empirical comparisons with states of known J and, for the higher l's ($l \geq 3$), a comparison with distorted wave calculations, confirmed the j- assignment to the $g_{9/2}$ hole state in ^{119}Sn.

More recently, this technique has been extended to the nuclei ^{208}Pb and ^{90}Zr. The experimental arrangement is similar to that described in reference 1. The experiment used a 90 MeV polarized proton beam from the Indiana cyclotron. The beam polarization was measured before injection into the final acceleration stage. Measurements every few hours throughout the three day run showed that the polarization was very stable gradually increasing from about 69% at the beginning of the run to 73% at the end of the run. The deuterons were detected in a pair of solid state detector telescopes. The Si ΔE detector was 2 mm thick and the intrinsic Ge detector 5 cm thick. To maximize the data taking rate, particle identification was carried out with a hard wired circuit which gave excellent particle identification (See Fig. 1) and allowed data to be recorded in a one dimensional mode only. Data rates of about 1.5 K cycle/sec were then possible with dead times of less than 10%.

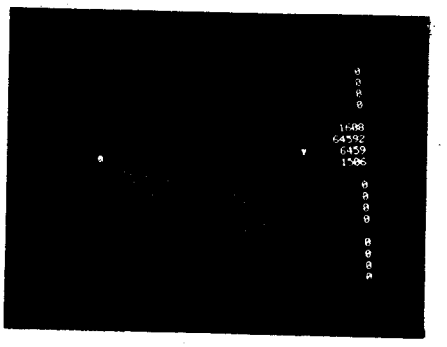

Fig. 1. Two dimensional display of the particle identifier versus energy. Groups seen correspond to protons, deuterons and tritons.

Spectra from ^{208}Pb, ^{90}Zr and ^{58}Ni at a laboratory angle of 14^{o} are shown in Fig. 2. By examining the spin up and spin down cases it is clear that there are significant asymmetries in these data. Of particular interest in the ^{208}Pb case is the separation of the $h_{9/2}$ and $h_{11/2}$ hole states. In ^{90}Zr, the assignment of $j = 7/2^-$ to the cluster of states near 5 MeV will be examined. The ^{58}Ni data which includes some known $f_{7/2}$ and $f_{5/2}$ hole states in ^{57}Ni, will provide an excellent empirical comparison for the ^{90}Zr case. These data are presently being analyzed.

---

* IUCF
** IPN, Orsay, France

1. G.M. Crawley, J. Kasagi, S. Gales, E. Gerlic, D. Friesel and A. Bacher, Phys. Rev. 23C, 1818 (1981).

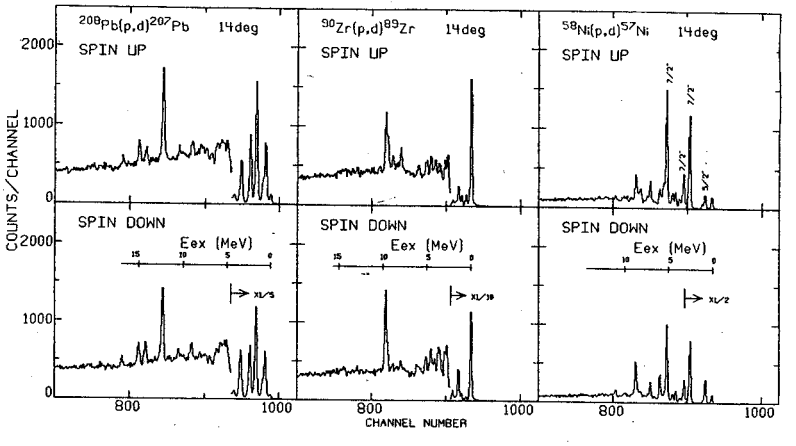

Fig. 2. Deuteron spectra obtained from ^{208}Pb, ^{90}Zr, ^{58}Ni(p,d) reactions at an angle of 14 deg.

Very Neutron - Deficient Nuclei in the Sn Region

D.C. Coyle and Wm. C. McHarris

For the past few years we have been studying the decays of short-lived nuclei in the very neutron deficient Sn region, using techniques of γ-ray spectroscopy aided by the "Helium-jet recoil-transport"system (He JRT).[1] This nuclidic region is of particular interest because nuclei far from stability (with large Q_ε values) populate states amenable to explanation in shell-model terms. There is also an abundance of isomeric states in this region, leading to the extensive population of both low and high-spin states. For example, many of the ground states involve $1g_{9/2}$ or $1g_{7/2}$ states, but there are also many nearby $1p_{1/2}$ states. And finally, we have found evidence for rotational bands in several of these nuclei, indicating the coexistance of spherical and deformed states within a relatively narrow energy range.

Activities were produced by bombarding a 90% enriched ^{106}CdO (natural abundance of ^{106}Cd is 1.3%) target with 30-75 MeV ^{3}He beams from the MSU 50 MeV sector-focused cyclotron. The activities were collected and transported within a few seconds to a low-background counting area by the He JRT. Extensive γ-ray singles, excitation function, E_γ vs time (for half-life measurements), and γ-γ-t coincidence experiments were performed, using a variety of Ge and Ge(Li) detectors and standard megachannel procedures[2] for listing on magnetic tapes.

Our analysis of these experiments/tapes is now nearing completion, with some confirmation of previous but much new information on states in In, Cd, and Ag, nuclides in the A = 102-106 region. Some sample experimental data are shown as follows: A singles γ-ray spectrum in Fig. 1, a specimen γ-γ coincidence gated spectra in Fig. 2, an excitation function in Fig. 3, and a half-life curve in Fig. 4.

The resulting decay schemes are shown in Figs. 5-12. Many straight forward shell-model states can be observed in these nuclides, especially the odd-mass In isotopes. But rotational bands can also be observed, e.g., in ^{105}Cd with states at 0, 832, and 1729 keV (J of $5/2^+$, $9/2^+$, and $13/2^+$ respectively). In addition, many odd-odd states in these nuclides have been characterized in shell model terms. In the end, because of the as yet incomplete analysis, we will not belabor the interpretation/analysis of states in these nuclei at this time. However, this can be found in the thesis of D. Coyle, which will be ready by the end of fall term, 1981 and also, in forthcoming publications expected within the next year.

---

1. K.S. Kosanke, M.S. Edmiston, R.A. Warner, R.B. Firestone, and Wm. C. McHarris, Nucl. Instr. Meth. 17, 78 (1975).
2. See e.g., R. Aryaeinejad, R.B. Firestone, W.H. Bentley, and Wm. C. McHarris, Phys. Rev. C, 23 194 (1981); or W.H. Bentley, Ph.D. Thesis, MSU, 1980.

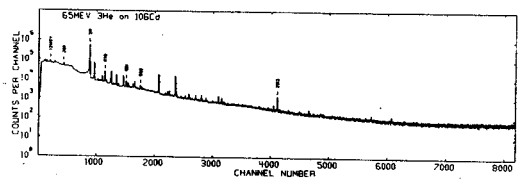

Fig. 1. γ-ray singles spectrum of 6.8-min ^{106}In taken with a 16% efficient true-coaxial Ge(Li) detector. This nuclide was produced by the ^{106}Cd(^{3}He,p2 n)^{106}In reaction at a beam energy of 65 MeV, and the data collected for 8 hours.

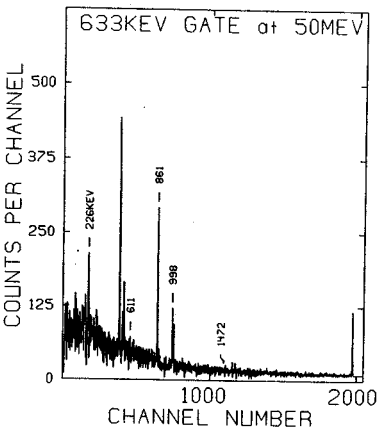

Fig. 2. Selected gates from γ-γ coincidence spectra for the decay of 6.8-min ^{106}In, taken with a 16% efficient true-coaxial Ge(Li) detector in coincidence with a 5% efficient intrinsic planar Ge detector. This nuclide was produced by the ^{106}Cd(^{3}He,2pn)^{106}In reaction at a beam energy of 50 MeV. The resolving time (2τ) was 50 nsec; and data was collected for 10 hr. for a total of 15 million total counts.

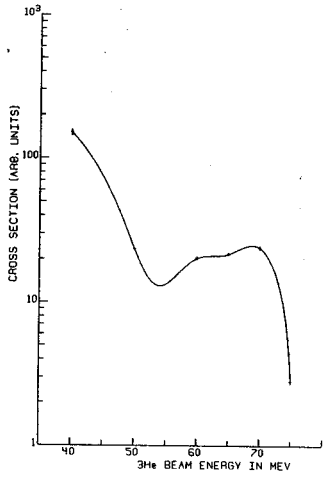

Fig. 3. Excitation function for 6.8-min. ^{106}In, which was obtained by following the 633 keV γ-ray.

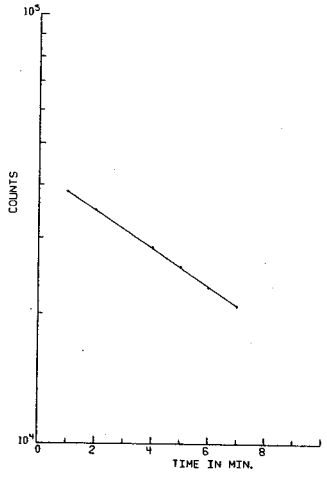

Fig. 4. Half-life determination for ^{106}In, obtained by following the 633 keV γ-ray from its decay. We obtain the value $t_{\frac{1}{2}} = 6.8 \pm 0.1$ min.

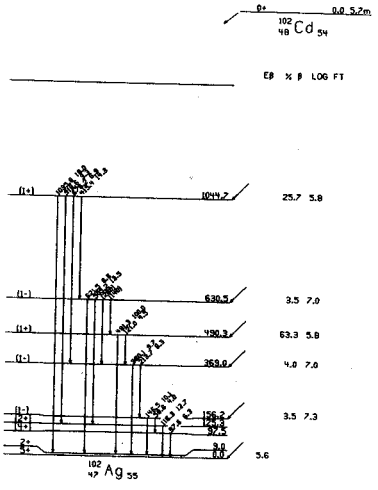

Fig. 5. Decay scheme of 5.7-min ^{102}Cd.

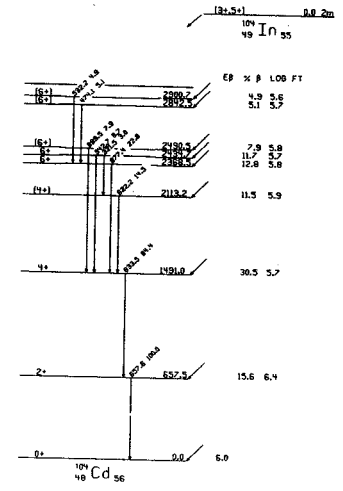

Fig. 6. Decay scheme of 1.8-min ^{104}In.

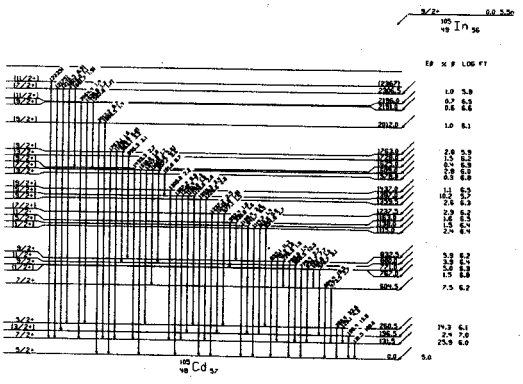

Fig. 7. Decay scheme of 5.5-min ^{105}In.

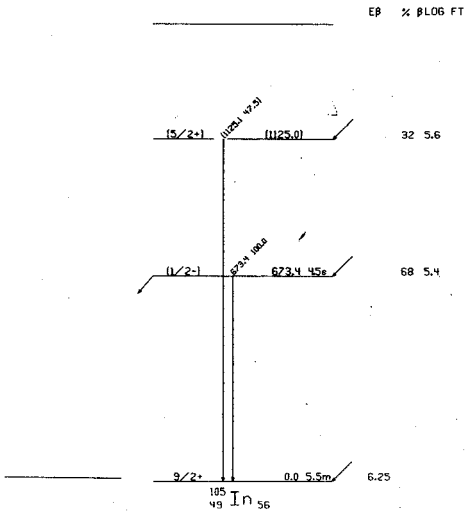

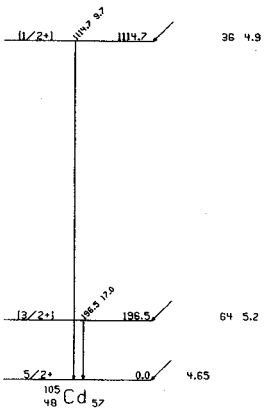

Fig. 8. Decay scheme of 45-sec. ^{105m}In.

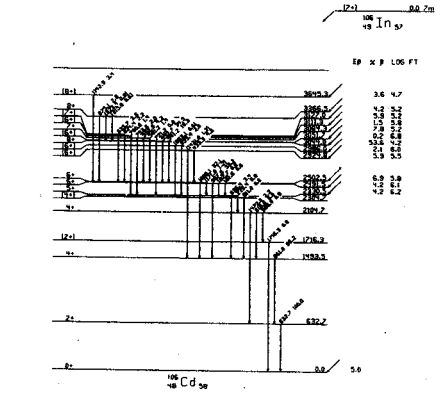

Fig. 9. Decay scheme of 6.8-min ^{106}In.

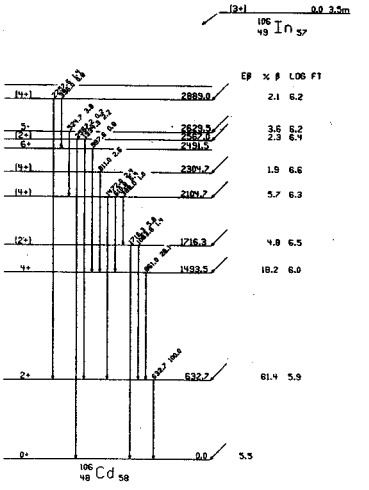

Fig. 10. Decay scheme of 3.5 min ^{106m}In.

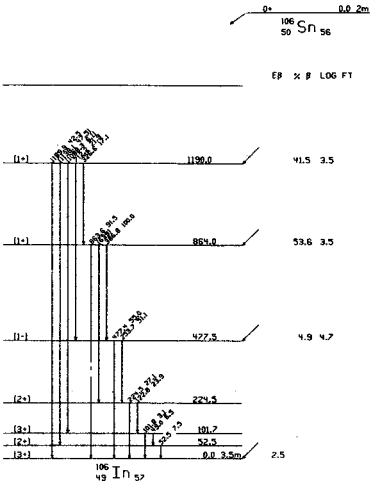

Fig. 11. Decay scheme of 2.0 min ^{107}Sn.

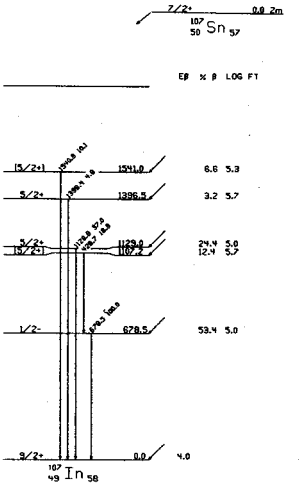

Fig. 12. Decay scheme of 1.9 min ^{106}Sn.

A Study of High-Spin States and Discrete Line Spectroscopy of ^{128}Ce

J.L.S. Carvalho, R.M. Ronningen, N.R. Johnson,* J.S. Hattula,** I.Y. Lee,* M.P. Fewell,*
L.L. Riedinger,*** H. Ower,*** J.C. Wells+ and F.M. Bernthal++

For the lighter even-even Ce isotopes a transition between spherical to prolate-deformed nuclear shape seems to occur as one moves away from the N=82 closed shell. This effects the sharpness of backbending and other phenomena of nuclear dynamics.

In order to better understand the nuclear behavior in this region, a series of studies was started at the Oak Ridge National Laboratory, and this collaboration is an extension of this program. The main goals were to study the high-spin levels and to determine any side-bands, side-feeding patterns and transition intensities in ^{128}Ce.

The reaction used was $^{112}Cd(^{20}Ne,4n)$ at about 103 MeV and a self-supporting, enriched foil target was employed. Seven Ge detectors, arranged around the reaction plane, were used in order to increase the number of coincident events into the 2-dimensional coincidence matrix. Two NaI detectors in near-4π configuration were placed above and below the target and served as a total γ-ray energy filter, in order to discriminate against different reaction channels. A multiplicity of at least four (three Ge, one NaI) was required for a coincident event, and these events were recorded on magnetic tapes for off-line analysis.

In the off-line analysis the total energy slices, corresponding to 5-particle and 4-particle evaporation, were used to separate the data into two 2-dimensional matrices and a master background subtraction technique was used to "clean out" the gated spectra from unwanted background contributed by continuum γ-rays. Further details on the analysis and the results will be submitted soon for publication.

---

* Oak Ridge National Laboratory, Oak Ridge, TN 37830.
** University of Jyväskylä, Finland.
*** University of Tennessee, Knoxville, TN 37916.
\+ Tennessee Technological University, Cookeville, TN 38501.
++ U.S. Senate, Washington, D.C.

Structure of ^{206}Pb from the (p,p') Reaction

J. Finck, G.M. Crawley, J.A. Nolen, S.M. Austin and R. Kouzes*

The strongest states excited by direct reactions in the doubly magic nucleus ^{208}Pb are the collective 3^-,5^-, 2^+, 4^+, 6^+, 8^+ levels between 2.5 and 5.0 MeV of excitation. Many experiments have been performed to examine the corresponding weak coupling states in ^{207}Pb (c.f. ref. 1 and references contained therein). Several experiments have also been performed on ^{206}Pb to observe the analogous collective states in this nucleus. These experiments show a strong correlation in both energy and strength of the collective states in the three nuclei with the exception of the L=5 states. We have performed an experiment using 35 MeV proton beams from the Michigan State and Princeton University Cyclotrons to examine these states in ^{206}Pb.

The angular distributions of the even parity states of ^{206}Pb are similar in shape to the corresponding states in ^{208}Pb, but the states of ^{206}Pb are all weaker by approximately 30%. The decrease in strength is not unexpected because of the increased level density in ^{206}Pb.

The angular distributions of the 3^- and 5^- collective states in ^{206}Pb are shown in Fig. 1. Two states at 3.193 and 3.515 MeV excitation energy, which were not previously identified as 5^- states, have angular distributions which are fit best by an L=5 shape. The L=4 calculation is also shown for comparison. The 3^- state at 2.648 MeV of excitation is the strongest excited state in ^{206}Pb and, like the even parity states, has a similar angular distribution with about 70% of the strength of the 2.615 MeV 3^- state in ^{208}Pb. However, the 5^- states in ^{206}Pb do not appear to follow the same trend as the other strong collective states.

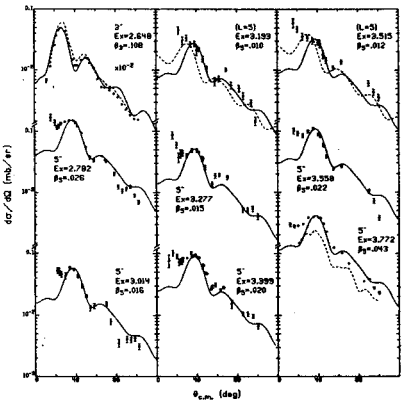

Fig. 1. Angular distributions for negative-parity excitations in proton scattering from ^{206}Pb. The solid lines represent collective DWBA calculations. The dashed lines shown with the 2.648 and 3.772 MeV states are interpolations of corresponding levels in ^{206}Pb.

It has been observed previously that the 5^- state in ^{206}Pb at 3.772 MeV of excitation probably corresponds to the 5^- state in ^{208}Pb at 3.709 MeV of excitation.[2] If this is true, this state is significantly stronger in ^{206}Pb. Indeed it is the strongest L=5 state seen in this ^{206}Pb(p,p') experiment. This is very different from the behavior of the other strongly excited collective states in ^{206}Pb.

It has also been observed that there is no analog to the 5^- state in ^{208}Pb at 3.198 MeV of excitation in either ^{206}Pb[4] or ^{207}Pb.[1] However, Wagner et al.[1] have observed six L=5 states in this region of excitation with 80% of the ^{208}Pb core strength. In Fig. 2 the levels of all three nuclei are plotted with their relative sgrengths shown. These results suggest a spreading of the L=5 strength in both ^{207}Pb and ^{206}Pb with only one or two neutrons removed from the ^{208}Pb core. We suggest that these phenomena can be explained by examining the wave functions of these states.

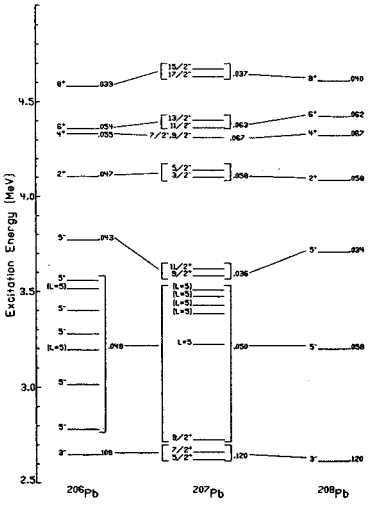

Fig. 2. Levels for which angular distributions were measured together with those measured in ref. 1. The numbers give the transition strength.

The wave functions of ^{206}Pb have been calculated and examined for the region below 2.6 MeV of excitation, but very little is known about the wave functions of the higher energy levels. Fortunately much work has been done in this energy region on the nucleus ^{208}Pb (c.f. ref. 3 and 4, and references contained therein). If we examine the 5^- state at 3.198 MeV of excitation in ^{208}Pb we find that the wave function has a large amplitude (0.8) neutron $lg_{9/2},p_{1/2}^{-1}$ component. The absence of the $p_{1/2}$ neutrons in ^{206}Pb appears to cause the spreading of L=5 strength. However, on the basis of the wave function, one should expect the L=5 strength to be reduced by much more than

the 20% observed due to the removal of $p_{1/2}$ neutrons. This suggests that the 5^- state in ^{206}Pb is more complicated and is not dominated by a $g_{9/2}, p_{1/2}^{-1}$ component. This behavior is similar to that observed in the $^{40}Ca - ^{48}Ca$ region.[6] Here both the 3^- and 5^- strengths were reduced and fractionated as one moved away from the closed $d_{3/2}$ shell and populated the $f_{7/2}$ shell with neutrons but again the decrease in the 5^- strength was less than expected on the basis of the particle-hole model.

The strength of the 5^- state in ^{206}Pb at 3.772 MeV of excitation compared to its corresponding state in ^{208}Pb can also be understood by examining the wavefunction of this ^{208}Pb state. This level has been shown to be a mixture of many configurations, none of which is dominant, and including a small amount of $p_{1/2}$ strength. One would then expect this state to behave like the other strongly excited states in ^{206}Pb. However, this state is significantly stronger in ^{206}Pb than in ^{208}Pb. This suggests that this state is gaining strength probably from the fractionated L=5 states at lower excitation energy. The total ^{206}Pb L=5 strength in this region is slightly less than the total strength of the two 5^- states in ^{208}Pb.

In summary, we have observed the strongly excited states in ^{206}Pb between 2.5 and 5.0 MeV of excitation. Accurate excitation energies and angular distributions were measured, and transition strengths have been determined. The even parity and 3^- states in the stable lead nuclei appear to be insensitive to any single particle structure. The 5^- states behave rather differently. When the core state in ^{208}Pb is principally dependent on the $p_{1/2}$ neutron single particle level, and these two neutrons are removed, the L=5 strength is fractionated and reduced. However the overall reduction in strength is similar to that observed for the other collective states implying that the 5^- wave functions are probably more complicated than those suggested by the simple shell model.

---

* Princeton University.

1. W.T. Wagner, G.M. Crawley and G.R. Hammerstein, Phys. Rev. C11 (1974) 486.
2. J. Alster, Phys. Lett. 25B (1967) 459.
3. W.W. True and C.W. Ma, Phys. Rev. C3 (1971) 2421.
4. H. Heusler and P. von Brentano, Ann. Phys. 75 (1973) 381.
5. W.T. Wagner, G.M. Crawley, G.R. Hammerstein, and H. McManus, Phys. Rev. C12 (1975) 757.
6. A.M. Bernstein and E.P. Lippincott, Phys. Rev. Letters 17 (1966) 321.

Multipole Moments of Deformed Nuclei from Intermediate Energy Inelastic Polarized Proton Scattering

R.M. Ronningen, N. Anantaraman, G.M. Crawley, B.M. Spicer, G.G. Shute, J.M.R. Wastell
D.W. Devins and D.L. Friesel

The reliable extraction of nuclear shape information from inelastic scattering with hadronic probes requires a detailed understanding of the reaction mechanism. A phenomenological analysis of the scattering can aid us greatly in understanding this mechanism. Recent studies[1,2] of proton inelastic scattering from deformed nuclei in the rare earth and actinide regions have employed a multipole moment analysis advocated by Mackintosh.[3] In this approach the data are fitted using a phenomenological deformed optical model potential. The multipole moments of the real part of the potential should be well determined and can be simply related[3] to the moments of the matter distribution under certain assumptions about the reaction mechanism. This method thus circumvents most model or reaction dependences, such as those which arise when comparing deformation parameters, or deformation lengths from experiments with different projectiles. If one assumes that the proton and neutron deformations are equal and that the nucleon-nucleon interaction is density-independent, the moments from proton inelastic scattering (properly normalized) should equal those from electron scattering and Coulomb excitation. If, on the other hand, the charge and matter moments are different, one or both of the assumptions above must be incorrect.

Many of the previous proton inelastic scattering experiments on deformed systems have been carried out at energies (such as those available from tandems) where there are significant Coulomb effects. A recent study[1] of ^{154}Sm, ^{176}Yb, ^{232}Th, and ^{238}U at MSU using 35 MeV protons indicated no large differences between moments extracted from proton scattering, electron scattering, and Coulomb excitation at least for the lower order moments, and showed that moments from proton inelastic scattering are in better agreement, in general, with the electromagnetic study results than those from α-particle scattering. Very recent studies[2] at LAMPF support the MSU work.

Few investigations of heavy, deformed systems have been made using energies between 35 MeV and 800 MeV. It is important to fill this gap for several reasons. First, inelastic proton scattering studies at intermediate energies on such nuclei as ^{12}C, ^{28}Si and ^{208}Pb have been analyzed[4,5] in terms of distorted-wave Born approximation calculations, whereas multistep processes have been shown to be important for ^{12}C and ^{24}Mg at both 35 MeV and 800 MeV. It will be valuable to investigate the importance of coupled channels effects as a function of bombarding energy in other deformed regions. In the rare-earth region, data exist at 35 MeV and 800 MeV and only a measurement at intermediate energies is needed to extend the data set.

Second, the 35 MeV data on the rare-earth nuclei are found to have some sensitivity to β_6 deformations. This sensitivity is expected to increase at intermediate energies, as indicated by coupled-channels calculations. The strength and structure of the 6+ angular distribution should yield a more reliable determination of the β_6 deformation parameter than was possible at 35 MeV. Thus, the higher order moments should be obtained more accurately than at 35 MeV.

Third, it is also important to precisely establish the systematic behavior of the moments as a function of energy. Recently Brieva and Georgiev[6] have calculated the deformed optical potential for proton inelastic scattering from a deformed matter density folded with a realistic internucleon force. They predict an energy dependence in the moments. The energy dependence is stronger for the hexadecapole and the hexacontatetrapole (6th order) moments than for the quadrupole moments and is especially strong for moments of the imaginary part of the potential.

Finally, little is known about the full importance of spin-orbit interaction effects in proton inelastic scattering from heavy deformed nuclei. Our earlier studies[1] at 35 MeV of deformed rare earth and actinide nuclei showed the need to include a spin-orbit interaction. Our latest study[7] showed that a spherical (no spin-orbit deformation) interaction was sufficient in fitting the angular distribution data. This is in contrast to proton scattering at 800 MeV where Ray[8] has shown that the inclusion of a spin-orbit interaction has only a small influence on fits of the angular distribution data. Near 135 MeV spin-orbit effects are large, and it has been shown[9,10] from a study of the ^{208}Pb(p,p') reaction that the spin-orbit form factors can have strikingly different deformations from the central ones. These differences show up in the analysis of angular distribution data for states with spins $J \geq 6$, and not when $J \leq 4$. This is in contrast to what is found[11] for lighter nuclei at lower incident energies. There the quadrupole deformation parameter in the spin-orbit interaction can be twice as large as in the central potential.

We have therefore begun a program of inelastic proton scattering on strongly deformed rare earth nuclei (^{154}Sm and ^{166}Er) to investigate these phenomena.

Elastic and inelastic scattering measurements were performed with a 134 MeV polarized proton beam from the Indiana University Cyclotron Facility using a helical-wire position-sensitive proportional counter in the focal plane of the QDDM spectrograph. The targets were metallic foils enriched in ^{154}Sm and ^{166}Er, and also ^{208}Pb for supplementary absolute cross section, optical model, and peak shape information. Angular distribution data for ground state rotational band states were measured at laboratory angles from 22.5° to 70° (^{166}Er) or 77.5° (^{154}Sm) in 2.5° steps. Two spectra are shown in Fig. 1. The resolution was typically 55 keV, this being sufficient for obtaining reliable peak areas after careful peak shape analysis. The data for the 6+ states show that the overall magnitudes of the cross sections for the two nuclei are quite different and that the respective angular distributions are out of phase for most of the angular range. All spectra are now being reduced to obtain cross sections and asymmetries. Coupled channels analysis will then begin.

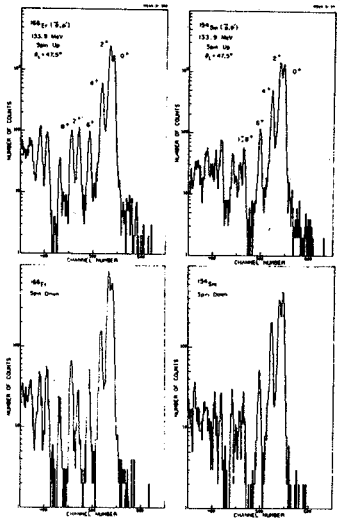

Fig. 1. Spectra from the ^{154}Sm, $^{166}Er(\vec{p},p')$ reaction at 134 MeV. Spin up and spin down data are shown for $\theta_L = 47.5$.

1. C.H. King, J.E. Finck, G.M. Crawley, J.A. Nolen, Jr., and R.M. Ronningen, Phys. Rev. C 20, 2084 (1979).
2. M.L. Bartlett et al., Phys. Rev. C 22, 1168 (1980).
3. R.S. Mackintosh, Nucl. Phys. A266, 379 (1976).
4. R.S. Henderson, et al., IUCF Technical and Scientific Report 1979, pp. 1-3.
5. S. Kailas et al., IUCF preprint (1980).
6. F.A. Brieva and B.Z. Georgiev, Nucl. Phys. A308 27 (1978).
7. R.M. Ronningen, R.C. Melin, J.A. Nolen, Jr., G.M Crawley and C.E. Bemis, Jr., MSUCL-353, 1981.
8. L. Ray, Phys. Lett. 102B, 88 (1981).
9. G.S. Adams et al., Phys. Lett. 91B, 23 (1980).
10. F. Petrovich et al., Phys. Lett. 91B, 27 (1980).
11. See J. Raynal, in The Structure of Nuclei (IAEA, Vienna, 1972), and references therein.

High Order Deformations of ^{232}Th and ^{234,236,238}U

R.M. Ronningen, R.C. Melin,* J.A. Nolen, Jr. G.M. Crawley and C.E. Bemis, Jr.**

We have completed the coupled channel analysis of ground band states in ^{232}Th, ^{234,236,238}U using (p,p') reactions at 35 MeV. The preliminary results were described in last year's annual report,[1] and recently a report[2] on the completed work was submitted for publication. To summarize, deformed optical model parameters (Table I) were extracted from the analyses of the elastic and inelastic scattering. It was found that a spherical spin-orbit interaction is sufficient for good fits to the angular distribution data. The deformation parameter β_6 is positive for ^{232}Th and ^{234}U, nearly zero for ^{236}U, and negative for ^{238}U. The multipole moments of the matter distribution were calculated as previously described and are also given in Table I. Quantitatively, the quadrupole and hexadecapole moments, q_{20} and q_{40}, differ from those deduced in Coulomb excitation[3] by nearly the same percentage differences as the differences between reduced proton and neutron moments calculated by Brack et al.[4] The qualitative trends the deformation parameters β_2, β_4, and β_6, and the multipole moments q_{20}, q_{40}, and q_{60} follow the predictions of a simple model by Bertsch.[5]

While preparing this report for publication we discovered that the name for the multipole moment q_{60} was misspelled. In our previous report "hexakontattetarapole"[6] was used. This should be spelled[7] "hexakontatettarapole", being derived from "ἑξήκοντα τέτταρα". However, to be consistent with the (latinized) spelling of "hexadecapole", we now adopt "hexacontatetrapole".

---

* Present address: Bell Telephone Laboratories, Murray Hill, NJ, 07974.
** Physics Division, Oak Ridge National Laboratory, Oak Ridge, TN, 37830.

1. R.C. Melin, R.M. Ronningen, J.A. Nolen, Jr., G.M. Crawley, C.H. King, J.E. Finck, and C.E. Bemis, Jr., MSU Annual Report, p. 13, 1980.
2. R.M. Ronningen, R.C. Melin, J.A. Nolen, Jr., G.M. Crawley and C.E. Bemis, Jr., MSUCL-253 (1981).
3. C.E. Bemis, Jr., F.K. McGowan, J.L.C. Ford, Jr., W.T. Milner, P.H. Stelson, and R.L. Robinson, Phys. Rev. C8, 1466 (1973).
4. M. Brack, T. Ledergerber, H.C. Pauli, and A.S. Jensen, Nucl. Phys. A234, 185 (1974).
5. G.F. Bertsch, Phys. Lett. 26B, 130 (1968).
6. R.S. Mackintosh, Rep. Prog. Phys. 40, 731 (1977).
7. C.H. King, private communication.

Table I. Deformed optical model parameters and multipole moments for ^{232}Th and ^{234,236,238}U from coupled channels calculations using a deformed (DSO) or a spherical (SSO) spin-orbit interaction.

Parameter	^{232}Th		^{234}U		^{236}U		^{238}U	
	DSO	SSO	DSO	SSO	DSO	SSO	DSO	SSO
V(MeV)	52.97	53.02	54.79	54.94	52.72	52.89	52.96	52.93
W_d(MeV)	4.96	4.86	5.31	4.84	5.36	5.12	4.48	4.02
V_{so}(MeV)	6.05	6.08	6.77	6.84	5.88	6.01	6.76	6.60
a_r(fm)	0.730	0.723	0.768	0.749	0.745	0.738	0.756	0.718
a_i(fm)	0.792	0.801	0.722	0.729	0.776	0.780	0.807	0.842
β_2	0.202(2)	0.204(2)	0.214(2)	0.210(2)	0.220(2)	0.218(2)	0.226(1)	0.226(2)
β_4	0.068(1)	0.067(1)	0.072(2)	0.072(2)	0.063(2)	0.060(2)	0.052(1)	0.047(2)
β_6	0.009(2)	0.010(2)	0.007(4)	0.007(4)	-0.003(5)	-0.003(5)	-0.011(1)	-0.013(1)
q_{20}(eb)	2.82(4)	2.85(4)	3.12(6)	3.05(6)	3.17(7)	3.17(7)	3.25(3)	3.20(4)
q_{40}(eb^2)	0.98(4)	0.97(4)	1.12(7)	1.09(7)	1.00(7)	0.99(7)	0.88(3)	0.79(4)
q_{60}(eb^3)	0.30(4)	0.31(4)	0.34(7)	0.33(7)	0.21(8)	0.21(8)	0.10(3)	0.06(3)

[a] In all calculations, W = 5.00 MeV, r_r = 1.17 fm, r_i = 1.32 fm, r_{so} = 1.01 fm, and a_{so} = .750 fm.

[b] In the case of ^{234}U and ^{236}U the values of β_6 used in the DSO calcualtions were obtained from the SSO "best fits". For ^{232}Th and ^{238}U the values of β_6 used in the DSO calculations were deduced from best fits to data adjusted for omission of the 8^+ state in the calculations. This involved comparing DSO calculations coupling 0^+ through 8^+ states with those coupling 0^+ through 6^+.

Levels in odd-odd ^{250}Bk populated by Alpha decay of $^{254}_{99}$Es

Z.M. Koenig, Wm.C. McHarris, I. Ahmad* and J. Milsted*

Level structure of ^{250}Bk has been investigated by measuring the alpha, conversion electron and gamma radiation following alpha-decay of 276-day ^{254}Es with high-resolution spectrometers. An essentially pure and mass-less source prepared in the Argonne electromagnetic isotope separator was used for these experiments. The alpha-particle spectrum was measured in the Argonne double-focusing magnetic spectrometer.[1] Energies, intensities and hinderance factors of alpha groups observed in the ^{254}Es spectrum are given in Table I.

The gamma-ray spectrum and conversion electron spectrum were measured with semi-conductor detectors in coincidence with alpha-particles. A three parameter-analyzer was used to record the alpha-particle energy, gamma-ray energy and the time difference between them with a time-to-amplitude converter in the event-by-event mode and recorded on magnetic tape. The tapes were latter played back with proper choice of windows in the parameter. The conversion electron spectra were used to determine the conversion coefficients and thus multipolarities. The multipolarities are shown in the skeletal level scheme (Fig. 1). The intensities of gamma-rays were measured in terms of photons per 100 ^{254}Es alpha-decays.

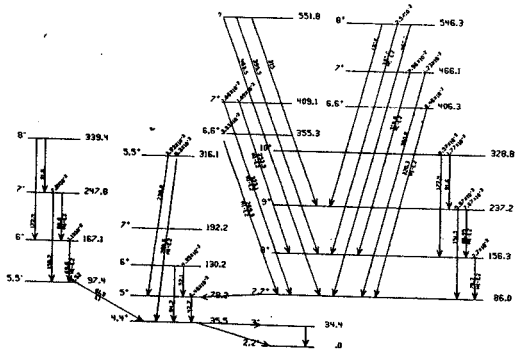

Fig. 1. The skeletal level scheme of ^{250}Bk.

The analysis to date has not been completed and a final scheme will be available in a forthcoming paper.

Table I. Data from the alpha spectra obtained by magnetic analysis.

Alpha-Particle energy (MeV)	Intensity (%)	Hindrance factor
6.512	2.5×10^{-3}	2.1×10^{5}
6.478	0.31	1.2×10^{3}
6.429	93.0	2.3
6.418	2.4	78
6.402	3.6×10^{-2}	4.4×10^{3}
6.385	0.15	8.8×10^{2}
6.361	3.1	33
6.349	0.84	1.1×10^{2}
6.326	4.6×10^{-2}	1.5×10^{3}
6.314	2.1×10^{-3}	2.8×10^{4}
6.281	0.17	2.4×10^{2}
6.270	0.22	1.7×10^{2}
6.254	9.0×10^{-3}	3.4×10^{3}
6.204	5.0×10^{-3}	3.4×10^{3}
6.192	1.5×10^{-2}	9.8×10^{2}
6.182	3.6×10^{-2}	3.6×10^{2}
6.166	3.0×10^{-2}	3.6×10^{2}
6.151	2.1×10^{-3}	4.4×10^{3}
6.115	0.54	11
6.092	7.4×10^{-2}	61
6.083	4.5×10^{-3}	9.0×10^{2}
6.060	0.18	17
6.051	2.1×10^{-2}	1.3×10^{2}
6.005	5.0×10^{-3}	3.2×10^{2}
5.982	9.7×10^{-2}	12
5.939	7×10^{-4}	1.0×10^{3}
5.928	1.7×10^{-3}	3.6×10^{2}
5.905	5×10^{-4}	9.2×10^{2}
5.892	9×10^{-4}	4.4×10^{2}
5.876	2.4×10^{-3}	1.3×10^{2}
5.856	5×10^{-4}	5.0×10^{2}
5.841	3.0×10^{-3}	69
5.816	1.1×10^{-3}	1.4×10^{2}
5.801	3×10^{-4}	4.1×10^{2}
5.793	5×10^{-4}	2.2×10^{2}

* Chemistry Division, Argonne National Laboratory, Argonne, IL.

1. I. Ahmad, H. Diamond, J. Milsted, J. Lerner and R.K. Stoblom, Nucl. Phys. A208 (1973) 287.